High sensitive malaria diagnosis using convolutional neural networks in an on-field setting

Riemer Sorgedrager[a]

[a] *Technical University Delft*

Abstract

This study focuses on automated malaria diagnosis in low quality blood smear images, captured by a low-cost smart phone microscope system. The aim is to localize and classify the healthy and infected erythrocytes in order to evaluate the parasitaemia of the blood. Due to the lower quality of the smartphone microscope system compared to traditional high-end light microscopes, conventional algorithms fail to process these images. We propose a framework using a convolutional neural network as a pixel classifier to localize the erythrocytes. Afterwards we classify them accordingly, using a convolutional neural network as an object classifier. Such a system can offer in-the-field malaria diagnosis without human intervention or can act as an aid for human experts to lower workload and increase diagnosis accuracy. The algorithm successfully localizes the erythrocytes with an average sensitivity of 97.31% and precision of 92.21%. Classification performed inadequate, in terms of low agreement with two human experts. This can due to the low image quality or the small amount of training data available at the time.

Keywords: Malaria Detection, Convolutional Neural Networks, Localization, Classification

1. Introduction

Malaria is a serious disease caused by a peripheral blood parasite of the genus Plasmodium. In 2015 alone, the global tally of malaria reached 212 million cases and 429 000 deaths. Most of these deaths occurred in the African region (92%) and the vast majority is due to P. falciparum malaria (99%) [1]. Early and accurate Malaria diagnosis and prompt treatment can cure a patient, preventing severe malaria cases and possible fatal disease states [1] [2]. All around the world there are still millions of people lacking access to malaria prevention and treatment [3].

Microscopy examination of Giemsa (or similar) stained thick and thin blood smears is regarded as the most suitable diagnostic instrument for malaria. It has numerous advantages, it is inexpensive, supports direct parasite count and discriminating different parasites. However, it requires skill and experience that is scarce even in developed countries [2][4].

Email address: r.sorgedrager@student.tudelft.nl (Riemer Sorgedrager)

Rapid Diagnostic Tests (RDTs) provide an alternative to microscopy. These ('dipstick') tests, also known as lateral flow immunochromatographic assays, are simple tests that allow detection of malaria antigens, and can be used by persons without diagnostic expertise [4]. To be a applicable diagnostic, RDTs must achieve greater than 95% sensitivity [5]. While most RDTs today can achieve this sensitivity for P. falciparum malaria, their results depend heavily on the storage, quality assurance and end user training. Despite some advantages, current RDTs are not intended to replace microscopy [6].

Light microscopy remains the gold standard for malaria diagnosis [6], however the manual inspection has numerous disadvantages. The costs of purchasing and maintaining microscopes are high [7]. Trained personal is scarce and also expensive since the technique is labour intensive and time-consuming [8]. The accuracy of this technique is ultimately determined by the expertise and reader technique of the microscopist and quality of the blood smear [9]. While theoretically very high sensitivity and specificity can be reached using microscopy analysis, practice shows big discrepancies between different technicians and on-field versus laboratory diagnosis results [9][10].

This current study is an extension to recent developments made by the Optical Smart Malaria Diagnosis (OSMD) project from the Technical University Delft. These developments include the substitution of a light microscope by a smartphone camera for the analysis of Giemsa stained thin blood smears [11]. This can mean drastic improvements to the cost, availability and readiness of malaria diagnosis in areas where proper equipment is limited or absent. Despite these advantages, the analysis of the blood smears is still done by human technicians. With the lack of proficient personnel and an image quality of smartphones that is inferior to that of light microscopes, these previously mentioned improvements are not exploited to their maximum.

Automated image analysis software could remove the most serious limitation of this system and microscopy in general, dependency on human expert performance for the diagnostic accuracy of the results. This software is not new, different image processing techniques has been applied in the past to tackle this problem. Most of these techniques are dedicated to the quantification of parasites with respect to the total amount of erythrocytes (red blood cells). Conventional techniques like morphology [12][13], edge detection [14], region growing [15] and more, have reported positive results with respect to their data. However all these researches are based on image data acquired using digital cameras coupled to light microscopes, examining Giemsa (or similar) stained thin blood smears under oil immersion. This data acquisition results in high resolution, highly detailed, uniform illuminated, altogether high quality images, and even in this type of images inconsistent light intensities is causing problems [13]. A low cost device using a smartphone camera to capture images will inherently produce inferior images, and these conventional techniques will not be sophisticated enough to analyze these images.

In this paper a novel approach to the automated malaria diagnosis problem is presented. We show a two-phase procedure to localize erythrocytes and classify them as healthy or infected in relative low quality thin blood smear images. Localization of the erythrocytes is done using a Convolutional Neural Network (CNN) as a pixel classifier, inspired on Cireşan's work on Mitosis detection [16]. The classification of individual erythrocytes is also done using

a CNN as an object classifier. The system must be able to provide a quantification and exact locations of healthy and infected erythrocytes shown in different field of views captured using the smartphone camera. Such a system would either enable a fully automated diagnosis or act as an aid to improve accuracy and lower workload of human experts.

The paper is organized as follows. Section 2 describes the specifications and differences of the acquired data using the smartphone camera and will show the performance of conventional algorithms on this data. Section 3 shows the two-phase approach using an Artificial Neural Network to localize erythrocytes and elaborates on the more conventional classification problem. In section 4 the experimental results can be found. Section 5 consist of the conclusion and discussion of this work.

2. Materials

Samples of malaria infected blood were obtained by Leiden University Medical Center, Leiden, Netherlands. All samples contain the Plasmodium falciparum parasite. Slides are placed in the smartphone set up and manually re-positioned to capture multiple fields of view. In total 120 images are taken, manually 40 images with the highest quality are selected and used for the research. The smartphone based microscope has specifications listed in table 1, as a comparison a standard light microscope used for malaria diagnosis is also listed. The smartphone based imaging platform consist of a Motorola Camera XT1572 with 20.7 megapixels camera sensor with a pixel size of 1.12 microns. Directly on the camera a 0.5 mm ball lens is placed, as explained in [11]. Images are captured in the JPEG format in the maximum resolution possible by the camera, 4080x5344 pixels. Since the imaging system has been optimized to minimize system aberrations, the usable field-of-view for the 0.5 mm ball lens is therefore limited to 100 microns (equivalent to approximately 1300x1300 pixels).

	Mag	NA	Dl Res	FOV
Standard Light Microscope	50x	1.25	0.22 μm	180 μm
Smartphone (0.5mm Ball Lens)	8.5x	0.2	1.8 μm	100 μm

Table 1: Specifications of smartphone based microscope system versus and a standard laboratory light microscope

Figure 1 shows a comparison between an example image captured using the smartphone set up and a digital camera coupled to a light microscope, taken from the Mamic Database used by Linder [17]. Both images show only the green colour channel in which the purple colour from stained parasites is most visible [13]. Big differences in illumination, contrast and detail (not visible at print-scale) can be found. These differences in quality can be explained by table 1. For the optimal quality the following applies; magnification, higher is better, numerical aperture, higher is better, diffraction limit resolution, lower is better, field of view, higher is better, but can be nullified by examining more field of views per sample. The smartphone is outperformed by the light microscope on all fronts by at least a factor 4, hence produces low contrast and low resolution images.

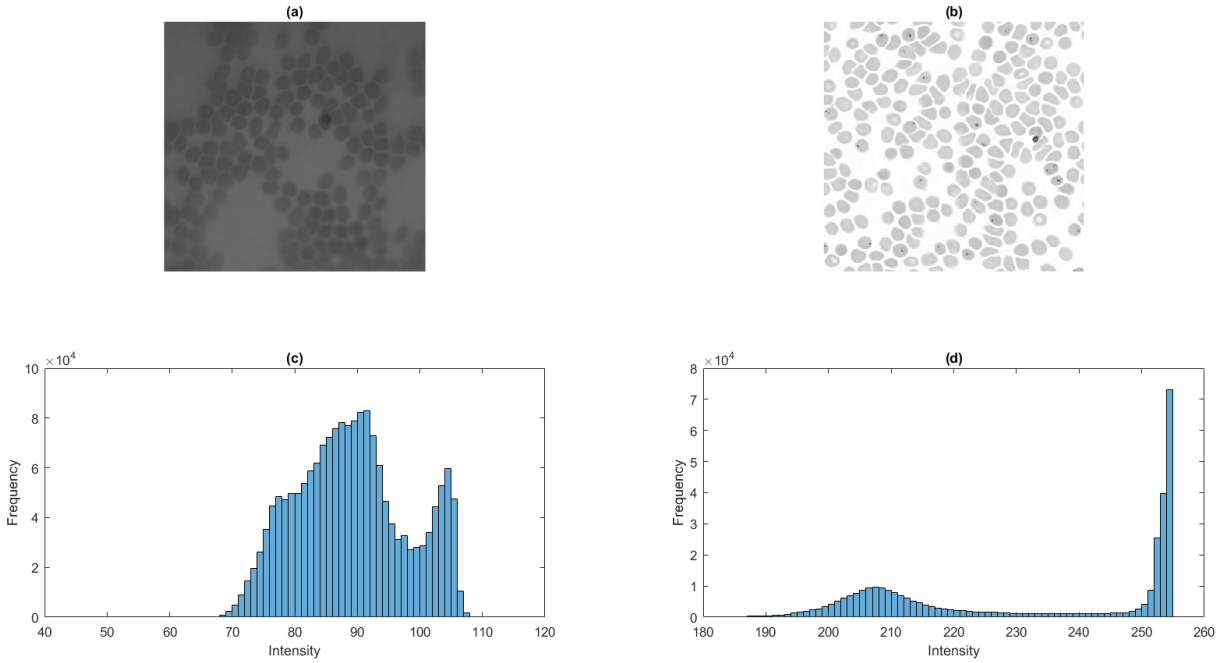

Figure 1: Example of smartphone image (a), with corresponding image histogram (c). Example of light microscope image, taken from Mamic Database (b) , with corresponding image histogram (d).

The differences in figure 1 also becomes clear looking at the distribution of the pixel value histograms. Histogram (d), corresponding to the light microscope, shows a typical bimodal histogram, the principal mode corresponds to the greyscale intensities of the background colour, and the second mode to those that make up the erythrocytes [13] [17]. Histogram (c), that of the smartphone image, shows a less distinct bimodal distribution. Most researchers, for example [13][17][12], use this distribution to their advantage, an easy way of segmenting the erythrocytes from the background is by selecting a threshold level that maximizes the separability of the resultant classes, this can be done automatically using Otsu's method [18]. The result of using this method on both examples from image 1 is shown in figure 2.

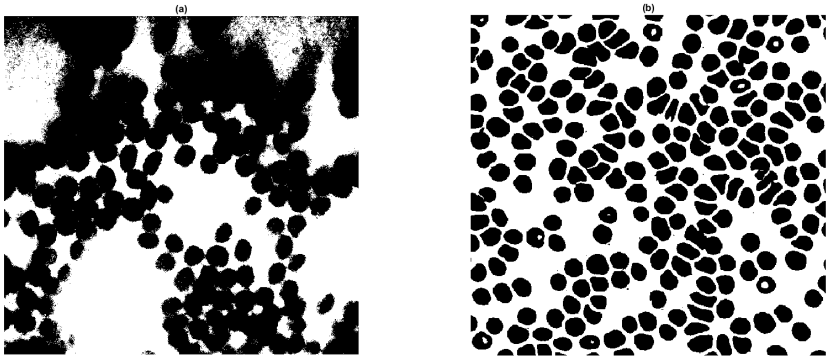

Figure 2: (A) Smartphone based microscope example image with Otsu's thresholding method. (B) Example image from a light micrsoscope taken from the Mamic Database with Otsu's thresholding method.

As can be seen in figure 2 the threshold method is not capable of segmenting all the erythrocytes from the background in the smartphone image. Due to a lack of uniform lightning, pixels that belong to erythrocytes in the top part of the image share the same intensity as the background in the lower part. Modern scientific light microscopy makes use of Köhler illumination, this illumination method results in extremely even illuminations, however, this increases the cost of the system. The smartphone set up is aimed to be very low cost and used a LED covered with a white paper, this can be improved a bit but will never reach the even distribution of Köhler illumination [19]. This result shown in figure 2 and the inherent lower quality of the smartphone set-up is the motivation for the use of more intelligent algorithms.

3. Method

Our proposed automated malaria diagnosis procedure consists of two stages: 1) Localization of all erythrocytes present in the image, 2) Classification of each found erythrocyte as either infected or healthy. Both phases are done using Convolutional Neural Networks, first as a pixel classifier, secondly as an object classifier. The results from the classification stage along with confidence scores for each classified erythrocyte can be shown for expert validation, afterwards parasitemia can be estimated. The overview of this process is shown in figure 3.

3.1. Convolutional Neural Networks

Convolutional Neural Networks (CNNs) is a class of deep, feed-forward Artificial Neural Networks specialized at analyzing image data [20]. After its introduction in 1980 [21] and early successes of digit classification in the 90's [22], these models have lately outperformed the well known algorithms for large-scale visual recognition and are widely adopted by industry giants as Google, Facebook and Baidu [23].

In the biomedical field CNNs are starting to make an impact as well, see Suzuki [24] for various examples. Segmentation of tissues in medical images is the basis of many image analysis applications developed for medical diagnosis [24].Many of these segmentation

problems are done by means of pixel classifiers. These problems are relatively simple due to the distinct appearance of the objects to be detected. Difficulties arise when objects are touching or clumped together and are harder to separate and identify [25]. In our case not only the clumped together erythrocytes pose problems, but due to the image quality the appearance of the 'same' object differs in different regions of a single image. Convolutional Neural Networks can deal with these problems with relative ease. Being able to 'learn' the features that make up the erythrocytes from raw RGB pixel values it can recognize the erythrocytes much in the same way humans do. This gives Neural Networks a certain versatility and high robustness against illuminance differences as well as clustering and overlap of objects.

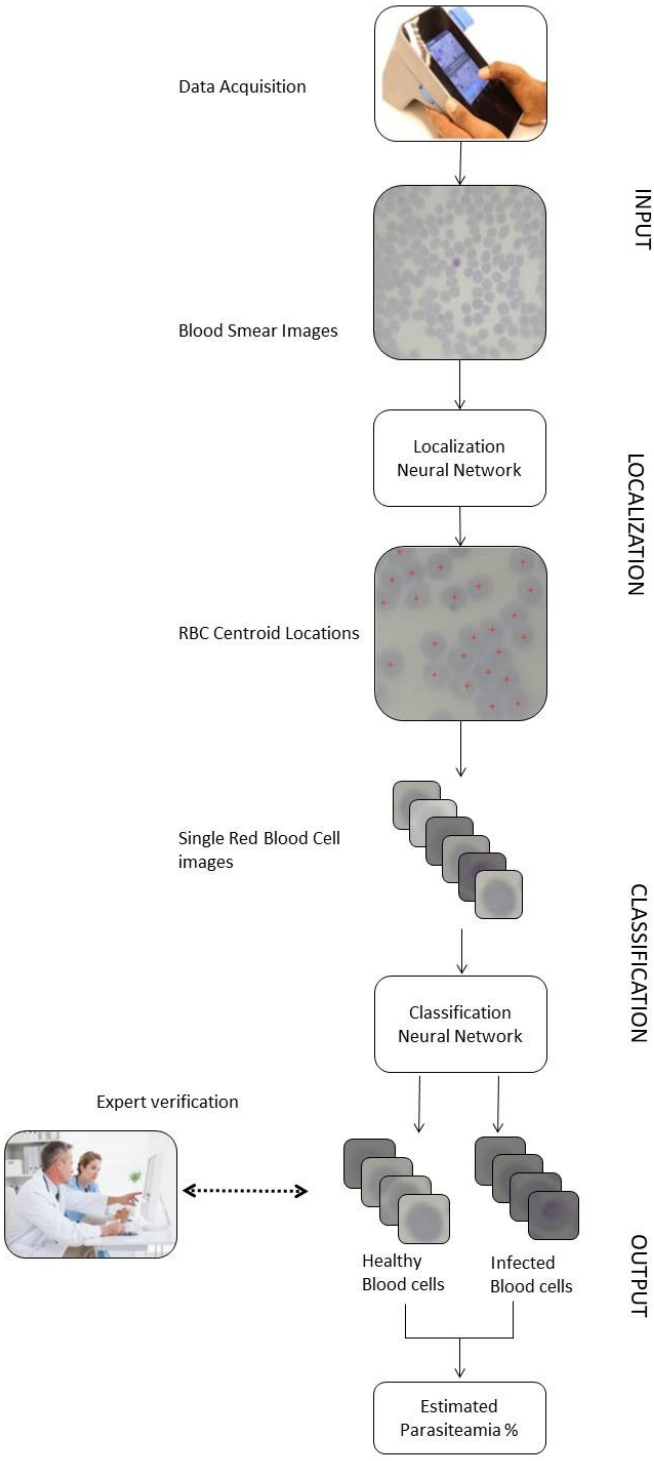

Figure 3: Overview of the proposed automated diagnostic method for the smartphone based microscope

3.2. Erythrocyte Localization

Given a RGB input image I the goal is to find the set $C = \{c_1, c_2, c_3, ..., c_n\}$ with elements c living in $\mathbb{R}^2$ and n is unknown beforehand. This set contains the centroid coordinates of all n erythrocytes present in I. To achieve this goal a CNN is trained to classify cropped images of I in two classes: *erythrocyte* or *non-erythrocyte*. The erythrocyte class should show one erythrocyte centred in the image with possible overlap or parts of others. The non-erythrocyte should show off-centre erythrocytes or no erythrocytes at all.

Using this CNN every pixel p in image I is classified, this process is shown in figure 4. This process is done by classifying small x by x windows of I that have pixel p as a centre and moves over every pixel p in I. At every pixel p the CNN computes the class for that specific window, stores this in a matrix and moves to the next pixel. After this process, every pixel p has a class designated and confidence matrix M can be constructed. This matrix depicts the confidence scores at every pixel for a specific class. For the first class, *erythrocyte*, we expect to see high scores (close to 1) around the erythrocyte centroids and low scores (close to 0) everywhere else. Using the post-processing steps explained in subsequent section 3.2.3 we can compute the set C from this matrix M.

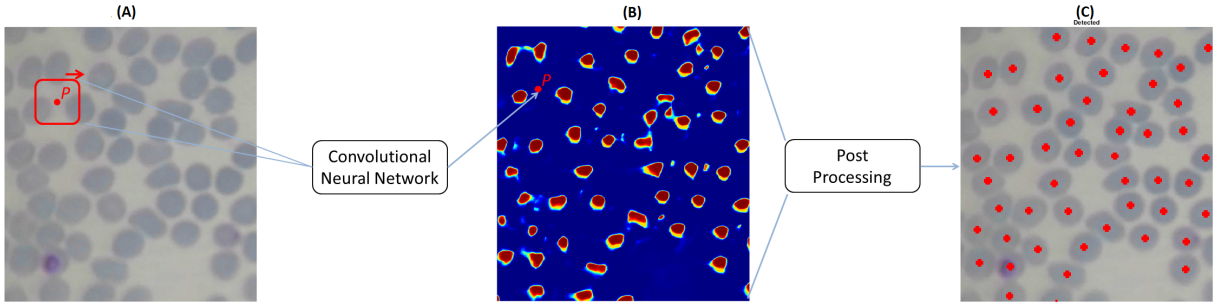

Figure 4: Localization process, (A) is a part of the input image, where p depicts the centre of the n by n window to be classified as erythrocyte or non-erythrocyte, (B) shows the confidence matrix M that holds output scores for one output class, (C) shows the centre locations found after post-processing the matrix M

3.2.1. Localization Network Architecture

We utilize a relatively narrow and shallow CNN for the localization phase, this is possible because of the simple shape of the erythrocyte that has to be detected. This network has to analyze very large amounts of data, a separate window for every pixel in I, so a small network is necessary to get acceptable computation times. The malaria infections, which are more detailed features inside the erythrocyte are only of importance in the second stage.

The network architecture is build up (from input to output) by 3 convolutional layers followed each by a max-pooling layer, hereafter 2 fully connected layers with a final double class softmax layer. Furthermore we use neurons with a ReLu activation function. This activation is a simpler computation compared to a traditional *tanh*, which requires computing an exponent. This results in decreased training and evaluation times[20]. Next to this, networks using ReLu activation usually result in sparse networks, sparsity in neural networks has various advantages, these are explained neatly by Glorot [26] in section 2.2 .

3.2.2. Training data

An expert manually annotated a total of 1473 erythrocytes centroids in 10 blood smear training images. To create a large enough training data set, 9 windows are cropped around each erythrocyte, the first window having its centre coincide with the annotation, and 8 others all shifted $+/-$ 1 pixel in either x or y direction. This results in a total of 13257 training images for the *erythrocyte* class.

For the *non-erythrocyte* class 13000 patches are randomly cropped from the same 10 blood smear images annotated by the expert. The only rule we impose on the these patches is that the center of a patch q can not be closer to a annotated centroid c by a euclidean distance of 20 pixels, i.e. $d(q_i, c_j) > 20 \; \forall \; i, j \in \mathbb{Z}$. This way we ensure that all non-erythrocyte training patches contain either off-centre erythrocytes or no erythrocytes at all.

Erythrocyte detection is rotational invariant. During each network training step we have a 50 % chance to augment the input image by rotating it 90 degrees, this should ensure a rotational invariance after training.

3.2.3. Processing an image

Localizing the erythrocytes in an unseen image I is straightforward at this point. Since the network learned the features of the erythrocytes on raw RGB values we do not have to do any preprocessing on a new image. Using the sliding window technique discussed before we get confidence matrix M, which yield the classification score for the erythrocyte class for every pixel p in image I.

To obtain set C we have to post-process the matrix M. First we threshold matrix M with a threshold level of 0.9, this leaves us with a new binary matrix that has value 1 for all areas where the network has a confidence of at least 90 % and a 0 every else. Secondly, we segment this binary image and split clumped areas with a watershed algorithm [27] on the binary matrix. Thirdly we calculate the centre of mass of all connected regions found by the watershed algorithm, these points make up the set C. At last we use our knowledge we have about the erythrocytes, due to their round shape we know the centres can not lie too close to each other. To ensure this we add a constraint to set C, that all points must have a minimum distance d_{min} from all other points. If two points lie too close to each other, both points are excluded from the set and a new point that is the average of both is added, this is done until the constraint is met. This yield final set C with all centroid coordinates.

Before the next phase we create a set of cropped images from I with the centre coordinates equal to those of the elements in C, if the algorithm was successful this set of images contain all erythrocytes present in I in separate images.

3.3. Erythrocyte Classification

Given the set of erythrocyte images derived from the localization step, the goal is to classify these as *infected* or *healthy*. To do this we use a CNN with a 2 class softmax output again, this is a straightforward classification problem discussed many times before and will not be discussed in detail.

The erythrocytes annotated by the expert before are divided in the *healthy* and *infected* class. Due to a small amount of blood smear training images, with relative low parasitemia,

the examples of infected erythrocytes are sparse. We have increased this data set by augmenting all sample windows, flipping them vertically to increase the data set by a factor 2.

The result of the classification yields two sets of images, set h with healthy erythrocytes and set i with the infected. The infected set and uncertain instances from the healthy set (with confidence scores around 0.5) can be shown to a human expert for validation. Incorrect classified instances can be added to the training database to improve the network performance over time. The parasitemia l can be derived by dividing the amount of images in the infected set by the total amount of images $l = n_i/(n_i + n_h)$.

4. Experimental Results

To asses the performance of our proposed method we will treat the algorithm as if it is a fully automated diagnostic tool, this means no human validation is used at the classification stage.

The algorithm is analyzed in two stages, the ability to localize the erythrocytes and the ability to diagnose an image, which means to estimate the parasitemia (amount of infected erythrocytes to total amount of erythrocytes).

Two human experts are shown 10 blood smear images captured by the smartphone . These images are enhanced using image editing software, where changes to brightness and contrast are made to make the parasites more visible for the human experts. Note that the original images are used for the algorithm evaluation. Expert 1 (5 years work experience) counted all erythrocytes manually using a tally counter, as if the image was viewed through a microscope. Expert 2 (4 months research experience) used computer software to manually annotate all erythrocytes and computed the counts from this. After counting, the amount of infected erythrocytes are determined by both the experts. After this manual step, the same 10 images, now annotated with all erythrocyte centroids having a red dot, is shown to the experts and verified as the ground truth. For the infections we are not able to establish this ground truth due to the poor image quality, uncertain cases will always persist even after careful inspections.

4.1. Localization Results

For the first stage, the ability to correctly localize the erythrocytes we will make use of two performance measures, the precision and sensitivity. Precision will depict the amount of erythrocytes among all identified spots by the network. Sensitivity will depict the amount of erythrocytes localized among all erythrocytes annotated in the ground truth image.

$$Precision = \frac{TP}{TP + FP} \qquad Sensitivity = \frac{TP}{TP + FN}$$

True positive (TP) is a localized centroid also annotated in the ground truth. False Positive (FP) is a localized centroid not annotated in the ground truth. False Negative (FN) is a centroid annotated in the ground truth but not localized by the network. For all these binary measures above, the hits and misses of the network, we stick to a small radius

around the annotated ground truth, if a localized centroid is close enough to an annotated centroid it 'hits' and count as a TP, if it too far off it 'misses' and counts as a FP.

It is of very high importance for us to have a high sensitivity since all found locations will be the input for classification stage, missed erythrocytes could mean missed infections. Besides, high precision is also needed to estimate the parasitemia correctly.

Results of the localization stage of all 10 images are shown table 2.

Table 2: Erythrocyte localization results of the algorithm against the ground truth for 10 images

Image #	Ground Truth Erythrocytes	Algorithm Detections	Precision	Sensitivity
1	151	150	98.00%	97.35%
2	149	155	94.84%	98.66%
3	132	132	96.97%	96.97%
4	185	193	94.82%	98.92%
5	87	96	90.63%	100.00%
6	77	81	90.12%	94.81%
7	93	104	85.58%	95.70%
8	129	141	87.23%	95.35%
9	141	146	96.58%	100.00%
10	128	140	87.14%	95.31%

The average precision has a mean of 92.21 % with a standard deviation of 4.60 %, the average sensitivity reaches a mean of 97.31 % with standard deviation of 1.99 %. As being said the sensitivity is the most important measure and scores on 9 out of 10 samples above 95 %, which is the lower bound to be an applicable diagnostic [5]. The precision is also reasonable. Most mismatches are found at areas where erythrocytes are clustered, which is a well known problem where other researches devote a lot of energy to [13]. This approach does not need extra steps to solve this problem, which is a nice advantage over other solutions. It can probably be improved by adding more training samples containing overlapped erythrocytes to the database.

4.2. Diagnostic Results

The results of the algorithm at diagnosing an image, which means first localizing the erythrocytes and afterwards classifying them accordingly is compared against the two experts. The results are shown in table 3, as an illustrative example the result of one of the images is shown in figure 5

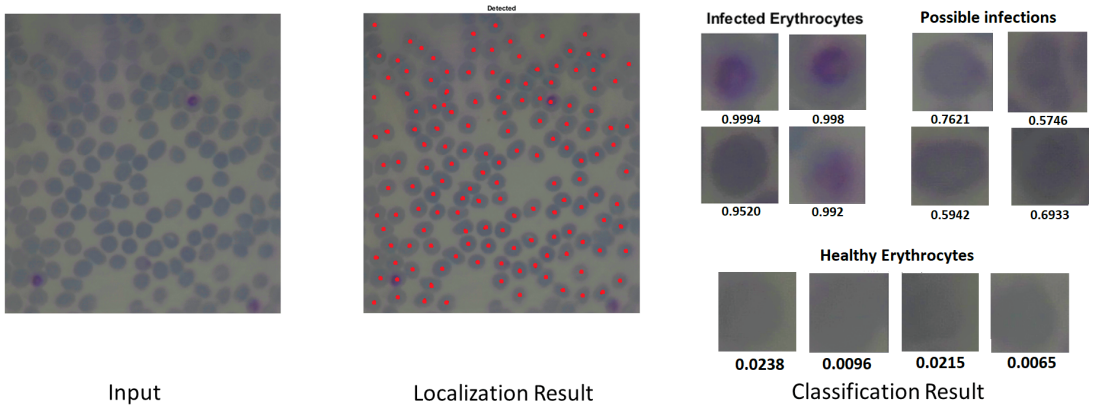

Figure 5: Erythrocyte localization and classification result of image 9, from left to right; the input image, the found centroid locations annotated with a red dot and a review of the classification result, showing the 4 infected erythrocytes (confidence scores greater than 0.9), 4 erythrocytes with possible infections (scores above 0.5 but below 0.9) and 4 examples of healthy erythrocytes with low scores, note that there are many more of these healthy erythrocytes but only 4 are shown in this figure

Table 3: Diagnosis Results of two human experts versus algorithm

	Amount of Erythrocytes			Infected Erythrocytes			Parasitemia		
Image #	Expert 1	Expert 2	Algorithm	Expert 1	Expert 2	Algorithm	Expert 1	Expert 2	Algorithm
1	112	150	150	3	3	1	2.68%	2.00%	0.67%
2	118	152	155	2	4	4	1.69%	2.63%	2.58%
3	116	134	132	1	4	3	0.86%	2.99%	2.27%
4	177	189	193	0	2	4	0.00%	1.06%	2.07%
5	81	88	96	1	2	5	1.23%	2.27%	5.21%
6	65	77	81	4	6	6	6.15%	7.79%	7.41%
7	91	94	104	3	4	5	3.30%	4.26%	4.81%
8	123	132	141	3	6	6	2.44%	4.55%	4.26%
9	125	143	146	2	5	4	1.60%	3.50%	2.74%
10	128	130	140	1	1	5	0.78%	0.77%	3.57%

To compare the results between the individual experts and the algorithm we observe the relation between the results of expert 1 (A), expert 2 (B) and the algorithm (C), for these we compute the covariance, correlation coefficient and the Root Mean Squared Error (RMSE) between A-B, A-C and B-C. The results are shown in table 4

Table 4: Diagnostic result comparison of expert 1 (A), expert 2 (B) and the algorithm (C). Relation between each participant is given by the covariance, correlation coefficient and Root mean Squared Error (RMSE). Relations are computed on the total number of erythrocytes annotated, total number of infected erythrocytes annotated and the estimated parasitemia from table 3

		Covariance	Corrrelation	RMSE
Erythrocytes	A-B	971.18	0.93	19.18
	A-C	953.80	0.96	22.09
	B-C	1100.87	0.99	6.31
Infections	A-B	1.56	0.73	2.02
	A-C	0.33	0.18	2.85
	B-C	0.77	0.30	1.90
Parasitemia (%)	A-B	0.03	0.90	1.40%
	A-C	0.02	0.65	2.08%
	B-C	0.03	0.73	1.45%

We already determined the erythrocyte localization performance against the ground truth, which gave good results. Compared to the experts it is also positive, from the results shown in table 4 we can conclude the correlation is stronger between the algorithm and the individual experts than the experts with each other, which indicates a nice in-between performance.

In the infection classification stage our performance is unfortunately deficient, looking at table 4. The scores are not enough in agreement with the human experts and are not acceptable for an automated diagnosis system. The foremost reason for this result could well be the size of the training data set, while there is no hard rule for a minimum dataset size, most neural networks start to perform well with a database of a few thousand samples per class [28]. We only have around 50 samples (not augmented) of infected erythrocytes in our database, acquiring more examples of infected erythrocytes should result in a better trained network with higher accuracy.

From closer inspection of the full results in table 3 we can see the algorithm has a excess of erythrocytes marked as infected, in 9 out of 10 cases compared to expert 1 and in 4 out of 10 compared to expert 2. This is essentially not a bad thing, proposed in figure 3 there is a possibility for human expert validation after the classification stage. We rather see the algorithm returning too much erythrocytes as infected which can be easily be checked and discarded by an expert than the algorithm missing infections.

5. Discussion and Conclusion

The recent developments by the OSMD project can mean a big improvement to the availability, readiness and costs of malaria diagnosis in low-resource areas. The low-cost smartphone based microscope system should enable in-the-field optical malaria diagnosis in areas where they currently lack proper diagnostic tools. But the diagnosis problem is a two-fold, not only proper equipment is lacking but experienced personnel is also scarce [7] [8] . The accuracy of optical malaria diagnosis is heavily dependent on the expertise and

reader technique of the microscopist. [9]. To overcome one of the biggest obstacles of this system and microscopy diagnosis in general, an automated diagnosis tool is proposed. Such a system is not new, various algorithms have been proposed for the quantification of parasites in stained thin blood smears [17][25][12][13] However, all these algorithms are based on high quality images captured using digital cameras coupled to high-end laboratory microscopes with extremely even illuminations due to Köhler illumination [19]. We have shown that the images from the low-cost smartphone based microscope are of too low quality to be analyzed with these conventional algorithms, and so the need for smarter algorithms arises.

In this thesis we presented an automated malaria diagnosis algorithm that analyzes smartphone acquired blood smear images. The problem is split in two stages, the first stage is to localize all erythrocytes so their locations and total number is known, hereafter in the second stage the erythrocytes are classified as either healthy or infected. This algorithm can serve as an independent diagnostic tool to calculate the parasitemia of a patient, which is an indication for the severeness of the disease. It can also serve as a diagnostic aid for human experts to lower workload and increase accuracy.

By posing the problem in such a way to enable the use of Convolutional Neural Networks for the localization of erythrocytes, the problems that arose due to low quality images with uneven lightning, were solved. Where previous studies used tools like morphological operators, as explained in section 2, these are shown to be insufficient for the smartphone images. The visual appearance of different erythrocytes in the same smartphone image differ too much as opposed to those from the high-end light microscope where all erythrocytes closely resemble each other. A Convolutional Neural Network is trained to recognize these different erythrocytes and to base its judgment on a deeper understanding of the shape, texture and colour of the erythrocyte rather than a difference in pixel intensity as a morphological threshold method would. Via this more advanced method, not only was the network able to localize the erythrocytes in the low quality images with a high average sensitivity of 97.31 % and precision of 92.21 %, but was also able to deal with clustered and overlapping erythrocytes without extra processing steps as other researches have implemented [17][25][12][13]. This provides a great perspective for the use Convolutional Neural Networks in the erythrocyte localization problem. Not only to employ this algorithm in the low-quality smartphone based microscope system. But also to work in an on-field setting where blood smears are often of sub-optimal quality compared to the laboratory setting most researches aim at.

The way we use the Convolutional Neural Network as a pixel classifier to localize multiple objects is not a common practice, actually is not to be found in the literature in this way. One of the downsides is the huge amount of data to be processed this way, where other researches use high quality, proper smeared blood samples the need for this more complex algorithm is absent. However, there is a lot of improvement to be made concerning efficiency. More efficient coding combined with pooling layers and the sparse network characteristic from the ReLu activations can mean very fast computing networks. Once these networks efficiency matches the conventional techniques they could provide benefits also for the high quality images. In sub-optimal quality blood smears that show more clustering or overlap of erythrocytes, we believe CNNs could provide the solution, however a detailed comparison using the same input data and different algorithms should prove this first.

The second phase, the classification of erythrocytes performed inadequate. The comparison with the human experts showed too little agreement, specifically, a correlation coefficient of 0.65 with expert 1 and 0.73 with expert 2 on the estimated parasitemia. Note must be made that the correlation of 0.90 between both experts is also considered quite low, as other researches report correlations between 0.97 and 0.99 [25] [29]. This lower correlation can be the cause of difference in experience between both the experts but is more likely to be the result of the low image quality, since both experts reported to feel uncertain in classifying particular erythrocytes due to the image quality.

On a positive note, the classification network annotated more erythrocytes as infected compared to the experts in 9 out of 10 cases compared to expert 1 and 4 out of 10 compared to expert 2. Closer inspection showed that the experts annotations were often subsets of the algorithms annotations. This is an encouraging result to use the network as an diagnostic aid, since the excess of infections can be easily checked by experts while still having confidence that no infections are missed by the algorithm.

The best result so far on erythrocyte classification is reported by Diaz [25], which classifies erythrocytes based on infections and also in life stages (ring/trophozoite or schizont infection). Diaz uses machine learning in the form of a SVM (support vector machine) and MLP (multilayer perceptron neural network) to perform the classification. A big difference with Diaz and a very probable cause for our lower performance is the size of our training data set, with only 50 (not augmented) samples of infected erythrocytes, compared to over 600 samples of Diaz, the training set is very small to train a CNN [28]. Another big difference is the image quality, with various luminance, smudged texture and edge distributions, and variations in saturation levels per individual erythrocyte from the same smartphone input image, the classification task becomes harder. We do believe convolutional neural networks could provide the outcome for this problem, especially Cirecsan, [30] shows promising results on the classification of traffic signs that deals with similar differences in detail and contrast using a multi-column deep neural network. Cirecsan has around 1000 training images per class. Future work should prove the increase in performance when using a larger training database. Also with an increase in size of the training database different possibilities open up for deeper convolutional neural networks, multi-column networks and other state-of-the-art solutions.

To conclude and summarize our contributions. We have investigated and proposed a solution to the diagnosis of malaria in low quality blood smear images. The quality of these images presented problems that conventional techniques of similar researches on automated malaria diagnosis could not solve. We have split the problem in two parts, first localization of erythrocytes and secondly the classification of these as healthy or infected. By using the framework proposed in this thesis, so that convolutional neural networks can be used for the localization of erythrocytes we believe to have found a suitable solution for the first part. The second part, the classification, is performing inadequate to serve as an automated diagnosis tool. Based on other sources in the literature, we do believe that the convolutional neural network provided here can offer the solution to this problem. Future work, with increased training databases and other improvements should prove this.

References

[1] WHO, World malaria report 2016, World Health Organization, 2016.

[2] L. Blumberg, J. Frean, Malaria control in south africa-challenges and successes, South African Medical Journal 97 (11) (2007) 1193–1197.

[3] WHO, Global Technical Strategy for Malaria 20162030, World Health Organization, 2015.

[4] C. Wongsrichanalai, M. J. Barcus, S. Muth, A. Sutamihardja, W. H. Wernsdorfer, A review of malaria diagnostic tools: microscopy and rapid diagnostic test (rdt), The American journal of tropical medicine and hygiene 77 (6_Suppl) (2007) 119–127.

[5] W. H. Organization, et al., New perspectives: malaria diagnosis. report of a joint who/usaid informal consultation, 25-27 october 1999., New perspectives: malaria diagnosis. Report of a Joint WHO/USAID Informal Consultation, 25-27 October 1999.

[6] D. Moonasar, A. E. Goga, J. Frean, P. Kruger, D. Chandramohan, An exploratory study of factors that affect the performance and usage of rapid diagnostic tests for malaria in the limpopo province, south africa, Malaria journal 6 (1) (2007) 74.

[7] C. C. Carpenter, G. W. Pearson, V. S. Mitchell, S. C. Oaks Jr, et al., Malaria: obstacles and opportunities, National Academies Press, 1991.

[8] B. S. Uzochukwu, E. N. Obikeze, O. E. Onwujekwe, C. A. Onoka, U. K. Griffiths, Cost-effectiveness analysis of rapid diagnostic test, microscopy and syndromic approach in the diagnosis of malaria in nigeria: implications for scaling-up deployment of act, Malaria Journal 8 (1) (2009) 265.

[9] W. P. O'Meara, M. Barcus, C. Wongsrichanalai, S. Muth, J. D. Maguire, R. G. Jordan, W. R. Prescott, F. E. McKenzie, Reader technique as a source of variability in determining malaria parasite density by microscopy, Malaria Journal 5 (1) (2006) 118.

[10] F. E. McKENZIE, J. Sirichaisinthop, R. S. Miller, R. A. Gasser Jr, C. Wongsrichanalai, Dependence of malaria detection and species diagnosis by microscopy on parasite density, The American journal of tropical medicine and hygiene 69 (4) (2003) 372–376.

[11] T. E. Agbana, J.-C. Diehl, F. v. Pul, S. M. Khan, M. Verhaegen, G. Vdovin, Imaging and identification of malaria parasites using cellphone microscope with a ball lens.

[12] C. Di Ruberto, A. Dempster, S. Khan, B. Jarra, Analysis of infected blood cell images using morphological operators, Image and vision computing 20 (2) (2002) 133–146.

[13] N. E. Ross, C. J. Pritchard, D. M. Rubin, A. G. Duse, Automated image processing method for the diagnosis and classification of malaria on thin blood smears, Medical and Biological Engineering and Computing 44 (5) (2006) 427–436.

[14] S. W. Sio, W. Sun, S. Kumar, W. Z. Bin, S. S. Tan, S. H. Ong, H. Kikuchi, Y. Oshima, K. S. Tan, Malariacount: an image analysis-based program for the accurate determination of parasitemia, Journal of microbiological methods 68 (1) (2007) 11–18.

[15] J. Theerapattanakul, J. Plodpai, C. Pintavirooj, An efficient method for segmentation step of automated white blood cell classifications, in: TENCON 2004. 2004 IEEE Region 10 Conference, IEEE, 2004, pp. 191–194.

[16] D. C. Cireşan, A. Giusti, L. M. Gambardella, J. Schmidhuber, Mitosis detection in breast cancer histology images with deep neural networks, in: International Conference on Medical Image Computing and Computer-assisted Intervention, Springer, 2013, pp. 411–418.

[17] N. Linder, R. Turkki, M. Walliander, A. Mårtensson, V. Diwan, E. Rahtu, M. Pietikäinen, M. Lundin, J. Lundin, A malaria diagnostic tool based on computer vision screening and visualization of plasmodium falciparum candidate areas in digitized blood smears, PLoS One 9 (8) (2014) e104855.

[18] N. Otsu, A threshold selection method from gray-level histograms, IEEE transactions on systems, man, and cybernetics 9 (1) (1979) 62–66.

[19] R. M. Society, Journal of the Royal Microscopical Society, Royal Microscopical Society, 1894.
URL `https://books.google.nl/books?id=0O4BAAAAYAAJ`

[20] A. Krizhevsky, I. Sutskever, G. E. Hinton, Imagenet classification with deep convolutional neural networks, in: Advances in neural information processing systems, 2012, pp. 1097–1105.

[21] K. Fukushima, S. Miyake, Neocognitron: A self-organizing neural network model for a mechanism of visual pattern recognition, in: Competition and cooperation in neural nets, Springer, 1982, pp. 267–285.
[22] Y. LeCun, B. E. Boser, J. S. Denker, D. Henderson, R. E. Howard, W. E. Hubbard, L. D. Jackel, Handwritten digit recognition with a back-propagation network, in: Advances in neural information processing systems, 1990, pp. 396–404.
[23] Y. Jia, E. Shelhamer, J. Donahue, S. Karayev, J. Long, R. Girshick, S. Guadarrama, T. Darrell, Caffe: Convolutional architecture for fast feature embedding, in: Proceedings of the 22nd ACM international conference on Multimedia, ACM, 2014, pp. 675–678.
[24] K. Suzuki, Artificial Neural Networks - Methodological Advances and Biomedical Applications, 2011.
[25] G. Díaz, F. A. González, E. Romero, A semi-automatic method for quantification and classification of erythrocytes infected with malaria parasites in microscopic images, Journal of Biomedical Informatics 42 (2) (2009) 296–307.
[26] X. Glorot, A. Bordes, Y. Bengio, Deep sparse rectifier neural networks, in: Proceedings of the Fourteenth International Conference on Artificial Intelligence and Statistics, 2011, pp. 315–323.
[27] F. Meyer, Topographic distance and watershed lines, Signal processing 38 (1) (1994) 113–125.
[28] D. C. Cireşan, U. Meier, J. Schmidhuber, Transfer learning for latin and chinese characters with deep neural networks, in: Neural Networks (IJCNN), The 2012 International Joint Conference on, IEEE, 2012, pp. 1–6.
[29] M.-T. Le, T. R. Bretschneider, C. Kuss, P. R. Preiser, A novel semi-automatic image processing approach to determine plasmodium falciparum parasitemia in giemsa-stained thin blood smears, BMC Cell Biology 9 (1) (2008) 15.
[30] D. Cireşan, U. Meier, J. Masci, J. Schmidhuber, Multi-column deep neural network for traffic sign classification, Neural Networks 32 (2012) 333–338.